JOURNAL OF MATERIALS SCIENCE 29 (1994) 1348–1351

Glass formation and crystallization of barium ferrite in the Na_2O–BaO–Fe_2O_3–SiO_2 system

C.-K. LEE, R. F. SPEYER
School of Materials Science and Engineering, Georgia Institute of Technology, Atlanta, GA 30332-0245, USA

Amorphous ribbons of approximate composition $0.13Na_2O$–$0.30BaO$–$0.30Fe_2O_3$–$0.27SiO_2$ were successfully fabricated using roller-quenching, after melting at 1400 °C. Devitrification of the amorphous phase by annealing at 710 °C for 2 h formed a uniform distribution of barium ferrite ($BaFe_{12}O_{19}$) particles with a mean diameter of 55.88 nm. Other crystalline phases formed on heat treatment were $BaFe_2O_4$ and $Na_2Ba_2Si_2O_7$. Devitrified ribbons showed a saturation magnetization (M_S) of 24.41 emu g^{-1} and a coercivity (H_C) of 3.06 kOe.

1. Introduction

The glass-crystallization method has been used in the synthesis of nanometre-sized barium ferrite ($BaFe_{12}O_{19}$) powder, since it has the advantage that no aggregates are formed. Crystallization of barium ferrite from a borate-based glass matrix was first attempted by Tanigawa and Tanaka [1], and has subsequently been reported by others [2, 3]. Borate-based glasses have a low resistance to moisture attack. This is advantageous when using this method for manufacture of particulate recording media, where the amorphous phase must be leached out. However, for thin film applications where the magnetic phase is dispersed in a glassy matrix, the matrix phase should not be vulnerable to moisture attack. These systems have also shown a propensity for inhomogeneous melting; haematite (α-Fe_2O_3) has formed in quenched ribbons when there was inadequate mixing during melting [4]. Haematite formed during quenching fosters growth of more haematite during devitrification heat treatment, suppressing nucleation and growth of barium ferrite. Barium ferrite can also crystallize on the surface of the ribbon during quenching. Under these conditions the particle size of surface-nucleated crystals is large, and a bimodal particle size distribution is observed after devitrification heat treatment of the quenched amorphous ribbons.

Phosphate-based glasses are known to be quite stable but do not form ferrites on devitrification. Various silicate, aluminosilicate and alumino-borosilicate-based compositions can be crystallized readily to form ferrites, partly during quenching and partly by annealing. This results in a crystal size and distribution dependence on sample geometry and dimensions [5]. Since the silicate-based compositions were selected using other intermediates, e.g. Al^{3+}, it is perceived that iron ions could not be easily accommodated into the amorphous structure, causing glass devitrification during quenching. Glass formation has been shown in the Na_2O–FeO–SiO_2 system when the silica content is high (e.g. ~ 75 wt %) [6].

In this study, the feasibility of controlled crystallization of barium ferrite in the silicate system Na_2O–SiO_2–BaO–Fe_2O_3 was investigated, and the results are compared with those in borate-based glass systems. In order to enhance the feasibility of iron ion incorporation in the quenched glass, no competing intermediate cations were added.

2. Experimental procedure

ACS grade Na_2CO_3, $Ba(OH)_2$, Fe_2O_3 and SiO_2 were used as raw materials. These chemicals were mixed with distilled water using a steel ball in a plastic bottle for 12 h. The selected batch compositions are summarized in Fig. 1 and Table I. Using a silicon carbide heating-element furnace, specimen compositions were melted in a Pt crucible, heated at 5 °C min^{-1} to 1400 °C (or 1450 °C for compositions j and k), and held for 4 h in a static air atmosphere. No mechanical stirring was used during melting. Amorphous samples were prepared by splat-cooling of the melt using two steel rollers, rotating at several hundred r.p.m. With this process, homogeneous amorphous ribbons were

TABLE I Chemical compositions chosen for study (initial mixing compositions)

Sample	Chemical composition (mol %)			
	Na_2O	BaO	Fe_2O_3	SiO_2
a	20	10	30	40
b	17	20	30	33
c	13	30	30	27
d	10	30	40	20
e	13	20	40	27
f	17	10	40	33
g	13	10	50	27
h	10	20	50	20
j	7	30	50	13
k	7	20	60	13

0022–2461 © *1994 Chapman & Hall*

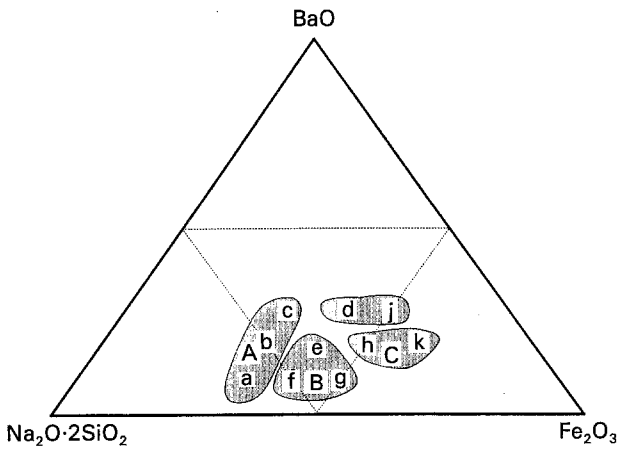

Figure 1 Selected chemical compositions in the Na_2O–SiO_2–BaO–Fe_2O_3 system (refer to Table I). By X-ray diffraction: (A) amorphous, (B) hematite and barium ferrite, (C) barium monoferrite and barium ferrite.

produced, as confirmed by X-ray diffraction (XRD) and transmission electron microscopy (TEM).

The thermal behaviour of the quenched ribbons was analysed by simultaneous thermal analysis (STA) combining differential thermal analysis (DTA) and thermogravimetry (TG) (Model 409, Netzsch Inc., Exton, Pennsylvania and Innovative Thermal Systems, Atlanta, Georgia) in a flowing air atmosphere with a flow rate of 100 $cm^3\ min^{-1}$. Crystallization thermal schedules entailed heating in a static air atmosphere at 10 °C min^{-1} from room temperature to 10 °C below a specified soak temperature, followed by heating at 2 °C min^{-1} to 610, 660, 710 and 760 °C, holding for 2 h.

The iron content and ferrous/ferric ratios were determined by wet chemical techniques with an accuracy of ± 0.1%. Crystallized samples were characterized using XRD, TEM and vibrating sample magnetometry (VSM). For XRD measurements, ground powder was distributed on the surface of a zero-background holder. XRD patterns were obtained (Philips Model 12405) using a step size of 0.02 °/step, and 2 s/step using CuK_α radiation. TEM samples were prepared by dimpling the divitrified ribbon with an oil-base diamond paste, and then ion milling with an argon plasma beam. A conductive carbon layer was then deposited on specimen surfaces. Particle size and aspect ratio were determined (Jeol JEM 2000-FX) by measuring the length and thickness of the particles showing lattice image fringing in TEM micrographs. It is expected that these fringes appear when the particle *c*-axis is nearly parallel to the imaging plane.

Magnetic properties of the crystallized samples were analysed using VSM (Model 155, EG & G Princeton Applied Research, Princeton, New Jersey). Specimens were loaded in a Pyrex tube of 3.0 mm i.d. and 4.0 mm o.d. In order to inhibit particle movement during measurement, particles were tightly packed and the tube was capped. Prior evaluation of the magnetization showed that the saturation magnetization was reached below 1500 Oe. Hysteresis loop behaviour therefore was determined by varying the field to 1500 Oe.

3. Results and discussion

3.1 Amorphous nature of quenched ribbons

Ribbons prepared by the roller-quenching method had a thickness range of 40 to 80 μm. Homogeneous amorphous ribbons were obtained by melting at 1400 °C when the amount of Fe_2O_3 was 30 wt %, which was confirmed by XRD and TEM analysis. The stable glass forming region is shown in area A in Fig. 1. The relative amount of BaO did not show any noticeable influence on the glass-forming tendency. However, the relative amount of Fe_2O_3 was crucial. Crystalline phases appeared in quenched ribbons if the amount of Fe_2O_3 was 40% or more. This range is comparable to that observed in a borate-based system, where 33 wt % Fe_2O_3 was the maximum content which still permitted stable glass formation upon quenching [2].

XRD results are summarized in Table II. In the iron-rich region (compositions f and g), haematite was present with a small amount of barium ferrite. With increasing barium content, barium monoferrite ($BaFe_2O_4$) and barium ferrite crystallized during quenching. Barium ferrite was present in most cases where the amorphous phase was not stable during quenching.

Wet chemical analysis showed that 4.3 mol % of iron ions were in the ferrous (Fe^{2+}) state, with the remainder in the ferric state, in as-quenched glass *c*. By comparison, in the borate-based system $0.100Na_2O$–$0.312BaO$–$0.258B_2O_3$–$0.330Fe_2O_3$, the quenched glass had 6.0 mol % of iron in the ferrous state [4]. Fe^{2+} or Fe^{3+} ions, which fall in the "intermediate" category in glass-forming, can function as either network-formers with a coordination number of 4 (tetrahedral), or network modifiers with a coordination number of 6 (octahedral), depending on the glass composition. Since iron ions have a higher field strength than Na^+ or Ba^{2+} [7–9], iron is prone to be a network-former rather than a modifier in this composition system, although a relatively small modifying contribution may be possible. In silicate glasses, Fe^{3+} functions as a network-former in conjunction with

TABLE II Crystalline phases forming in the quenched ribbons before and after devitrification at 760 °C (all samples melted at 1400 °C except j and k which were melted at 1450 °C)

Sample	Crystalline phases in glass[a]	Crystalline phases for devitrified sample[a]
a	None	s N2Ba2S, s Ba6F,
b	None	s N2Ba2S, m Ba6F, w unin2
c	None	s N2Ba2S, s Ba6F, s unin2
d	s unin 1	s N2Ba2S, m Ba6F, tr F
e	w Ba6F	s N2Ba2S, m Ba6F
f	m F, w Ba6F	w Ba6F, tr N2Ba2S
g	s F, w Ba6F	s F, m Ba6F, tr N2Ba2S
h	s BaF, tr Ba6F	s N2Ba2S, m Ba6F, m BaF
j	m Ba6F, w N2Ba2S	s N2Ba2S, s Ba6F
k	s BaF, s Ba6F	s N2Ba2S, s Ba6F

[a] Peak intensity is a relative comparison amongst amorphous and devitrified samples, separately: (s) strong, (m) medium, (w) weak, (tr) trace; (F) α-Fe_2O_3, (BaF) $BaFe_2O_4$, (Ba6F) $BaFe_{12}O_{19}$, (N2Ba2S) $Na_2Ba_2Si_2O_7$, (unin) unidentified phase(s).

modifying Na^+ or Ba^{2+} ions. However, Fe^{2+} adopting a network position requires two monovalent modifiers. In borate glasses iron can either be a network former by direct substitution of Fe^{3+} for B^{3+}, or Fe^{2+} can be a glass-former in conjunction with either Na^+ or Ba^{2+}. During quenching, ferrous iron tends to oxidize to the ferric form. The greater stability of Fe^{2+} in a borate-based system might be expected to translate into a higher percentage of this ion remaining in the quenched glass (compared to a silicate-based system), as was observed.

No ferrous ions were found after crystallization in either borate- or silicate-based systems, which implies that ferrous iron in the glass was fully oxidized during the crystallization heat treatment. Thermogravimetric analysis of a borate system confirmed that reoxidation occurred at about 500 °C [2]. The presence of the ferrous ion in the as-quenched glass is thus not expected to influence devitrification.

3.2. Devitrification behaviour

STA analysis (2 °C min^{-1}) of the quenched ribbon of composition *c* showed a glass transition (T_g) of ~ 520 °C. XRD analysis of samples heat-treated to various temperatures indicates that sodium barium silicate ($Na_2Ba_2Si_2O_7$) formed first after heat treatment at 610 °C. Then, barium ferrite ($BaFe_{12}O_{19}$) and an unidentified phase formed after heat treatment at 660 °C. Finally, barium monoferrite ($BaFe_2O_4$) formed after heat treatment at 710 °C. The $BaFe_{12}O_{19}$ crystallization temperature of composition *c* was higher than in the borate system ($0.100Na_2O$–$0.312BaO$–$0.258B_2O_3$–$0.330Fe_2O_3$), which was below 600 °C [4], but lower than that after using chemical co-precipitation [10, 11], where ferromagnetic behaviour became evident only after heat treatment at 740 °C. For the chemical co-precipitation case [11], haematite formed first, then barium ferrite devitrified at higher temperature.

The crystalline phases formed after devitrification at 760 °C for various silicate based compositions, determined by XRD, are listed in Table II. Regardless of the relative amount of chemical constituents, and of the crystallinity of the starting quenched ribbons, in most compositions, barium ferrite and sodium barium silicate were the predominant devitrified phases. This contrasts with the borate-based system in which barium ferrite formed only in a limited phase field, and haematite or magnetite (Fe_3O_4) were major crystalline phases [1]. Haematite appeared in this silicate-based system when the amount of Fe_2O_3 was high (region B in Fig.1). Barium monoferrite or sodium barium silicate became prominent as the BaO, Na_2O and SiO_2 contents were increased.

For a magnetic glass–ceramic, a homogeneous amorphous state in the quenched ribbon and a large amount of magnetic crystals after devitrification are desirable. Composition *c* in this study, which showed three crystalline phases (barium ferrite, sodium barium silicate and an unidentified phase) best fitted this criterion.

Devitrification studies involved heating to specified temperatures with a two hour soak period.

No noticeable crystal growth was found after heat treatment of composition *c* at 610 °C. However, after treatment to 660 °C, the mean devitrified crystal size was 48.58 nm with an aspect ratio 8.02. Crystallization heat treatment at 710 and 760 °C showed mean crystal sizes of 55.88 and 52.35 nm with aspect ratios of 7.36 and 7.55, respectively. These values, however, are all located within a standard deviation of the measurements taken. These results imply that crystallization largely terminated at ~ 660 °C, and that further heat treatment did not alter the microstructure.

In the case of devitrification of crystalline species of different composition to that of the parent glass, crystal growth occurs via diffusion of constituents from the surrounding glass. The depletion of required constituents ultimately limits crystal growth, often prior to mutual impingement. Because individual crystals are separated by a vitreous silicate matrix, no grain growth would occur as when thermally treating a polycrystalline mass. The dissolution of small crystals and coarsening of large crystals would be a mechanism of abnormal crystal growth in the glass-crystallization method. However, this is not expected because of the high viscosity of the matrix and the corresponding low atomic solubility and diffusivity of chemical species from the small crystals in this temperature range.

A representative TEM micrograph of the devitrified microstructure is shown in Fig 2. The figure shows a uniform distribution of barium ferrite crystals after devitrification at 710 °C for 2 h. The optimum size range for use in data storage applications is ~ 50 nm, with an aspect ratio of 3 to 7 [12]. The size range obtained in this work is therefore, within the optimum range, although a somewhat larger aspect ratio was measured.

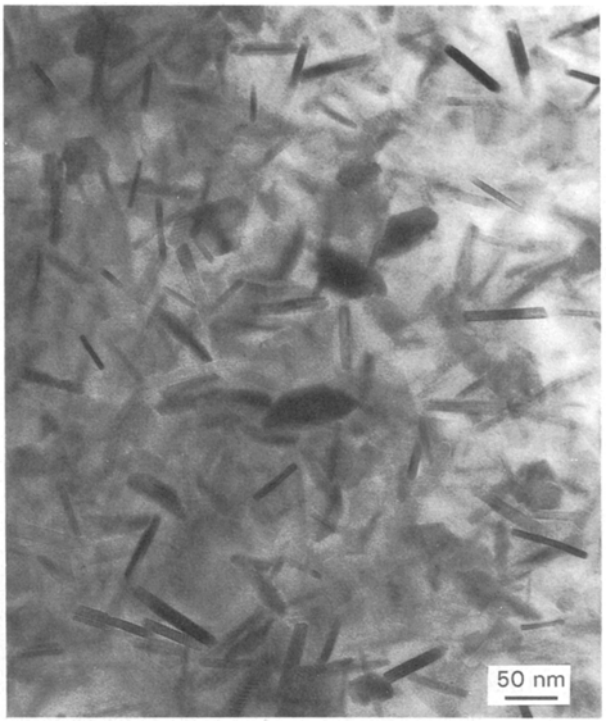

Figure 2 TEM microstructure of a quenched ribbon of composition *c* after crystallization at 710 °C for 2 h.

3.3. Magnetic properties

Fig. 3 summarizes the magnetic properties obtained from compositions *b* and *c* devitrified at 610, 660, 710 and 760 °C for 2 h. Both samples heat-treated at 610 °C showed paramagnetic properties, while those crystallized at 660 °C or above, demonstrated ferromagnetic properties. Saturation magnetization and coercivity values did not show an apparent change with crystallization temperature above 660 °C, which matches well with that expected based on their microstructures. Typically, the samples crystallized at 710 °C had a saturation magnetization (M_s) of 24.41 emu g^{-1}, a coercivity (H_c) of 3.06 kOe, and a squareness (M_r/M_s) of 0.51. A typical hysteresis loop behaviour of a sample of composition *c* heat-treated at 710 °C is shown in Fig. 4.

Coercivity increases with particle size in barium ferrite for diameters under 1 μm. Saturation magnetization depends not only on particle size and shape, but on the amount of magnetic phase relative to that of non-magnetic phase [13]. Therefore, saturation magnetization can be a measure of the relative amount of barium ferrite in the glass–ceramic. Kubo *et al.* [3] reported that the saturation magnetization of pure barium ferrite is 58 emu g^{-1} with a coercivity of 0.9 kOe. This specimen was prepared using the glass-crystallization method with a borate-based system where the amorphous phase was removed by acid leaching. Average particle dimensions were 80 nm in diameter and 30 nm in thickness. Based on their saturation magnetization, the glass–ceramic of composition *c* studied herein is calculated to contain ~ 41 wt % of barium ferrite.

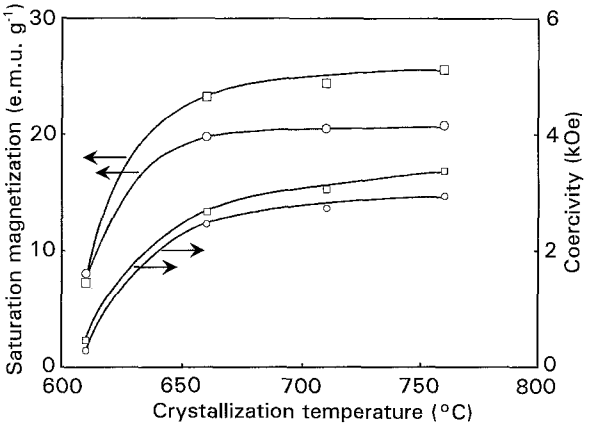

Figure 3 Saturation magnetization and coercivity of the crystallized samples depending on the devitrification temperatures: (○, o) composition *b* (□, □) composition *c*.

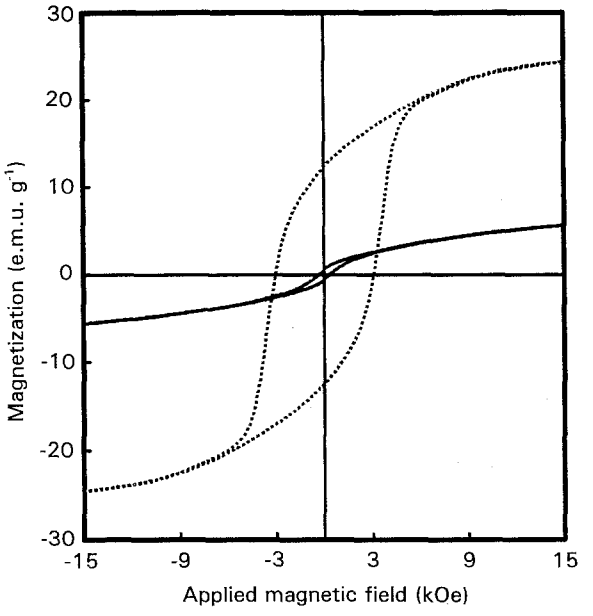

Figure 4 Typical hysteresis loop behaviour of the crystallized composition *c*, heat-treated at (——) 610 °C and (···) 710 °C.

4. Conclusions

Formation of amorphous ribbons and subsequent devitrification behaviour was studied in the Na_2O–SiO_2–BaO–Fe_2O_3 system. A homogeneous glass was formed for compositions in the range of $0.13Na_2O$–$0.27SiO_2$–0.30BaO–$0.30Fe_2O_3$. After devitrification at 760 °C, the predominant crystalline phases formed were sodium barium silicate ($Na_2Ba_2Si_2O_7$) and barium ferrite ($BaFe_{12}O_{19}$). Crystallization of the quenched ribbon with the above composition at 710 °C for 2 h gave a uniform distribution of barium ferrite crystals, having an average size of 55.88 nm and an aspect ratio of 7.36, which is appropriate in applications for particulate magnetic recording. This glass–ceramic showed a saturation magnetization of 24.41 emu g^{-1} and a coercivity of 3.06 kOe.

Acknowledgements

The authors would like to gratefully acknowledge Ms Yolande Berta for transmission electron microscopy work and Mr Gerry Cartledge for wet chemical analyses.

References

1. H. TANIGAWA and H. TANAKA, *Osaka Kogyo Gijutsu Shikenso Kiho* **15** (1964) 285 (in Japanese).
2. B. T. SHIRK andW. R. BUSSEM, *J. Amer. Ceram. Soc.* **53** (1970) 192.
3. O. KUBO, T. IDO and H. YOKOYAMA, *ibid.* **Mag-18** (1982) 1122.
4. C. K. LEE and R. F. SPEYER, Presentation 6-EP at 94th Annual Meeting of American Ceramic Society, Minneapolis, MN, 1992, manuscript in preparation.
5. A. HERCZOG, *The Glass Industry* (August 1967) 445.
6. M. B. VOLF, "*Chemical Approach to Glass*", Glass Science and Technology, Vol. 7 (Elsevier, New York, 1984) p. 347.
7. A. DIETZEL, *Glastechn. Ber.* **22** (1948/49) 41.
8. *Idem, ibid.* **22** (1948/49) 81.
9. *Idem, ibid.* **22** (1948/49) 212.
10. K. HANEDA, C. MIYAKAWA and H. KOJIMA, *J. Amer. Ceram. Soc.* **57** (1974) 354.
11. W. ROOS, *ibid.* **63** (1980) 601.
12. T. FUJUWARA, *IEEE Trans. Magn.* **Mag-21** (1985) 1480.
13. *Idem, ibid.* **Mag-23** (1987) 3125.

Received 18 February
and accepted 28 July 1993